Analysis of Artifactual Components Rejection Threshold towards Enhanced Characterization of Neural Activity in Post-Stroke Survivor

Mojisola Grace Asogbon, Yaping Huai, Samuel Oluwarotimi Williams, Zhengxiang Jing, Yixin Ma, Jingyu Liu, Yibo Jiang, Yunfa Fu, Guanglin Li*, Yongcheng Li*

***Abstract*— Research advancement has spurred the usage of electroencephalography (EEG)-based neural oscillatory rhythms as a biomarker to complement clinical rehabilitation strategies for motor skill recovery in stroke patients. However, the inevitable contamination of EEG signals with artifacts from various sources limits its utilization and effectiveness. Thus, the integration of Independent Component Analysis (ICA) and Independent Component Label (ICLabel) has been widely employed to separate neural activity from artifacts. A crucial step in the ICLabel preprocessing pipeline is the artifactual ICs rejection threshold (TH) parameter, which determines the overall signal's quality. For instance, selecting a high TH will cause many ICs to be rejected, thereby leading to signal over-cleaning, and choosing a low TH may result in under-cleaning of the signal. Toward determining the optimal TH parameter, this study investigates the effect of six different TH groups (NO-TH and TH1-TH6) on EEG signals recorded from post-stroke patients who performed four distinct motor imagery tasks including wrist and grasping movements. Utilizing the EEG-beta band signal at the brain's sensorimotor cortex, the performance of the TH groups was evaluated using three notable EEG quantifiers. Overall, the obtained result shows that the considered THs will significantly alter neural oscillatory patterns. Comparing the performance of the TH-groups, TH-3 with a confidence level of 60% showed consistently stronger signal desynchronization and lateralization. The correlation result shows that most of the electrode pairs with high correlation values are replicable across all the MI tasks. It also revealed that brain activity correlates linearly with distance, and a strong correlation between electrode pairs is independent of the different brain cortices.**

***Clinical Relevance:* This study indicated that optimal selection of the ICLabel artifactual rejection threshold is essential for EEG enhancement for adequate signal characterization. Thus, a TH-values with a confidence level between 50% - 70% would be suggested for artifactual ICs rejection in EEG.**

I. INTRODUCTION

Recent development in stroke rehabilitation has brought about the use of brain oscillatory patterns as potential biomarkers for recovery prediction and treatment response in post-stroke survivors. Also, existing works have established that the fusion of motor system modulation and rehabilitation strategies further aids the recovery process in upper limb post-stroke survivors [4-6]. Over the years, EEG (Electroencephalography) neuroimaging technique has been widely utilized to measure/ quantify motor response in the human brain due to its non-invasiveness, easy setup and acquisition procedure, high temporal resolution, portability, and cost-effectiveness [7]. Despite its advantages, an unpreventable challenge with EEG is that it contains a mixture of signals (brain and non-brain activities) from multiple sources, thereby resulting into signal misinterpretation [8]. For this reason, EEG preprocessing pipeline has become essential in achieving quality brain signals. A blind source separation technique based on Independent Component Analysis (ICA), has been notably applied to separate independent sources from linearly mixed EEG signals obtained via multiple channels. Specifically, ICA reconstructs the sources into new mixtures such that the actual brain source will be enhanced in some components and the artifacts in others [9]. The application of ICA in EEG preprocessing has been beneficial; however, manual inspection is conventionally utilized in recognizing and rejecting independent components (ICs) after decomposition. For accurate and proper ICs analysis, adequate time and practice are required to study their properties, since ICs have no specific order or clearly defined interpretations [10-11].

The emergence of data- driven approaches and machine learning models have led to the development of automated ICs recognition and elimination methods, including MARA, ADJUST, FASTER, SASICA, IC_MARC, and ICLabel for ICA decomposition optimization [10-11]. ICLabel, a deep learning-based model, has demonstrated superiority in terms of improved accuracy and faster computational time compared to other approaches [11]. ICLabel, developed by Luca Pion-Tonachini et al., is an EEG-based IC classifier trained on an extensive database of expert labeling of ICs, classifying the ICs into seven classes consisting of the brain, muscle, eye, heart, line noise, channel noise, and others (unclear sources), thus allowing the removal of artifactual components in a consistent manner[11]. In recent time, many studies have employed ICA to separate neural sources from artifactual sources, and ICLabel for ICs identification and rejection. For instance, RELAX (Reduction of Electroencephalographic Artifacts), a recently developed automated EEG artifact removal implemented in EEGLAB utilized ICLabel for artifact components detection [12]. A study conducted by [13] investigated the efficacy of an EEG-based brain-computer interface virtual reality system for post-stroke upper limb rehabilitation. In their signal preprocessing, the combination of manual inspection and ICLabel were used for ICs labeling

The research work was supported in part by the Ministry of Science and Technology of China under grants (STI2030-Brain Science and Brain-Inspired Intelligence Technology-2022ZD0210400), National Natural Science Foundation of China under grant (#62150410439), Basic Research Project of Shenzhen Science, Technology and Innovation Commission (#JCYJ20210324123414039), and The Scientific Research Projects of Medical and Health Institutions of Longhua District, Shenzhen（#2020040).

M.G. Asogbon, O.W. Samuel, Z.X Jing, Y.X Ma, G. Li and Y.C Li are with the CAS Key Laboratory of Human-Machine Intelligence-Synergy Systems, Shenzhen Institutes of Advanced Technology (SIAT), Chinese Academy of Sciences (CAS), Shenzhen, Guangdong 518055, China (Dr. Yongcheng Li, email: li.yc@siat.ac.cn; Dr. Guanglin Li, phone: 86-755-86392219; fax: 86-755-86392299; e-mail: gl.li@siat.ac.cn) .

O.W. Samuel is with School of Computing and Engineering, University of Derby, Derby, DE22 3AW, United Kingdom

Y.P. Huai, J.Y Liu and Y.B Jiang are with the Department of Rehabilitation Medicine, Shenzhen Longhua District Central Hospital, Shenzhen, Guangdong, 518000, China.

Y.X Ma and Y.F Fu are with the Department of Information Engineering and Automation, Kunming University of Science and technology, 650031, Yunnan, China

and rejection. While these studies and many more have used ICLabel either for only ICs detection/ detection and rejection, minimal or no information has been provided on the ICLabel artifactual components rejection threshold (TH) utilized in their studies. The components rejection TH is one of the crucial steps in the ICLabel pipeline that determines the number of ICs to be eliminated. It is presumed that a high TH value will cause large ICs to be rejected, possibly leading to signal over-cleaning (loss of brain signal), and choosing low TH value may result to under-cleaning of the signal (retaining more artifacts). For this reason, some researchers tend to reject only a few components mostly related to eye and muscle artifacts. Besides, total separation of the brain signal from artifacts is challenging, thus selecting appropriate TH value for the ICs classes is highly essential in other to obtain clean signals that reflect requisite neural activity and is almost/nearly free of artifacts. In this regard, this study systematically investigated the effect of varied ICLabel based artifactual component rejection employing different TH values on EEG signal recorded from post-stroke patients who performed four distinct MI tasks including wrist and grasping movements. The performance evaluation of each TH group was compared with data without component rejection (NO-TH) using three standard EEG quantifiers, including brain topographical map that employs z-scored power, Pearson correlation coefficient, and classification accuracy.

II. METHODS

A. Participants information

A total of six ischemic stroke patients with no other neurological or psychiatric disease were recruited to participate in the MI tasks experiment designed for the study. Two out of the patient have an intracranial skull. The demographic information of the patients is presented in the table below (Table 1). The participants agreed to the objective of the study and gave written informed consent and permission for the publication of their data to improve scientific knowledge. The experimental protocol was approved by the Institutional Review Board of Shenzhen Institutes of Advanced Technology, Chinese Academy of Sciences, and Shenzhen Longhua District Central Hospital (NO. SIAT-IRB-220715-H0601).

Table 1: The participant's demographic information

Patient Number	*Age (Years)*	*Sex*	*Paretic Limb*	*Level of Impairment*	*Time of Stroke (months)*
P1	76	F	Left	2	36
P2	37	M	Left	2	3
P3	41	M	Left	1	2
P4	60	M	Left	0	2
P5	56	M	Left	0	2
P6	52	M	Right	0	2

B. Data Acquisition and Preprocessing Pipeline

The study experiment was conducted at the Department of Rehabilitation Medicine, Shenzhen Longhua District Central Hospital. A 64-channel EEG recording system (EasyCap Brain Products GmbH, Germany) was utilized to record the signal from the participants. The EEG electrode channels were distributed over the scalp of each patient based on the international 10–20 electrode placement configuration, as shown in Fig. 1A. The impedance was kept below 5 kΩ and 8kΩ depending on the patient tolerance level. The MI-EEG signals were recorded at a sampling rate of 1000 Hz and referenced to CPz during recording. Before the commencement of the experiment, the patients were briefed and trained to get them accustomed to the experimental procedure. As presented in Fig.1B and 1C, five out of the six participant's elicited four MI tasks consisting of key grip (KG), power grip (PG), wrist extension (WE), and wrist flexion (WF) during the experimental session. Participant 1 (P1) was able to perform only three tasks (PG, WE and WF). During the experiment, a computer screen was placed in front of the participants to play a video of each MI task. The video contained 10 images of active (say, key grip) and 10 images of non-active (rest) tasks making 20 total tasks per video. The participants were instructed to imagine eliciting the corresponding MI task displayed on the screen when the video is been played. Each active task in the video is displayed for 5s, followed by a 5s rest period to avoid mental fatigue. All participants did two experimental sessions for each MI task. It is worth noting that the EEG acquisition system was integrated with TTL parallel synchronization box via a custom-built MATLAB script to automatically create a marker on the EEG recordings at the onset points of each specified MI task, triggered when a corresponding motor task appears/disappears on/from the computer screen.

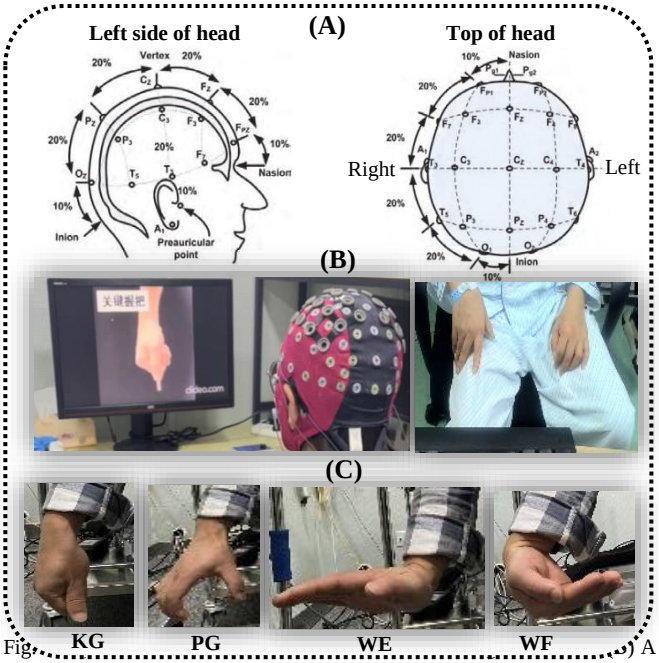

Fig. 1. (A) A representative patient during one of the experimental sessions (C) Pictorial representation of the motor imagery tasks including wrist and grasping movements

The preprocessing and analysis of the recorded MI-EEG data were performed using EEGLAB (version 2022.0) and MATLAB (version R2018b) toolboxes. Meanwhile, studies [4, 15] have reported beta oscillations as a potential biomarker in stroke recovery since they are involved in cortical disinhibition and associated with sensorimotor processing. Therefore, the beta frequency band in the range of 16-26Hz was extracted from the recorded signal using a spectrogram-

based short-time Fourier transform and eighteen channels located (including FC1, FC2, FC3, FC4, FC5, FC6, C1, C2, C3, C4, C5, C6, CP1, CP2, CP3, CP4, CP5, and CP6) at the sensorimotor cortex region (ROI) of the brain was used for the investigation in this study.

C. ICLABEL Artifact Rejection Threshold parameter

In this study the default version of ICLabel that uses IC spectrum, topography, and autocorrelation activities as features for classification was utilized due to its better estimation of brain ICs. The ICA decomposition technique was applied to the filtered signal using INFOMAX and ICLabel was employed to classify/label the ICs. Subsequently, a threshold value with minimum and maximum limits is selected to flag the components for rejection. Since one of the primary determinants of the preprocessed signal outcome is the artifact rejection TH value applied to the classified ICs, this study investigates six different TH groups (Table 2) on MI-EEG signal recorded from stroke patients. The performance of the TH groups was compared with EEG signal recorded without applying ICLabel and is denoted as NO-TH. Afterward, the active segment of each TH group data was epoched from -1 to 5 and save for subsequent analysis.

Table 2: Probability range (Min-Max) to flag components for rejection

Artifacts/ Noise	Threshold Confidence level (Min - Max)					
	40% (TH-1)	50% (TH-2)	60% (TH-3)	70% (TH-4)	80% (TH-5)	90% (TH-6)
Eye	0.4 - 1	0.5 - 1	0.6 - 1	0.7 - 1	0.8 - 1	0.9 - 1
Muscle	0.4 - 1	0.5 - 1	0.6 - 1	0.7 - 1	0.8 - 1	0.9 - 1
Heart	0.4 - 1	0.5 - 1	0.6 - 1	0.7 - 1	0.8 - 1	0.9 - 1
Line	0.4 - 1	0.5 - 1	0.6 - 1	0.7 - 1	0.8 - 1	0.9 - 1
Channel	0.4 - 1	0.5 - 1	0.6 - 1	0.7 - 1	0.8 - 1	0.9 - 1
Other	0.4 - 1	0.5 - 1	0.6 - 1	0.7 - 1	0.8 - 1	0.9 - 1

D. Feature extraction and MI tasks decoding

For adequate decoding of the MI tasks, the preprocessed signal was portioned into different analysis windows using an overlapping technique of 1s window length with an increment of 100ms. Following this, wavelet transform, a time and frequency domain feature often used in the space of EEG signal characterization [16], was extracted and used to construct a machine learning model based on linear discriminant analysis (LDA), to decode the four MI tasks. The LDA classifier was trained and tested using a 5-fold cross-validation scheme to circumvent model biasedness.

E. EEG evaluation quantifiers and statistical analysis

Three quantifiers namely z-score based topographical map (TM), correlation coefficient (CC) given in Eq. 1 and average classification accuracy (ACA) shown in Eq. 2 were utilized to analyze performance between the NO-TH and TH groups.

$$Accuracy_{ave} = \frac{\sum_{i=1}^{N}\left(\frac{TP_i+TN_i}{TP_i+FN_i+FP_i+TN_i}\right)}{N} \quad (1)$$

where N is the number of MI classes, TP_i: true positive, FP_i: false positive, FN_i: false positive, and TN_i: true negative.

The CC between two random variables X and Y with nonzero variation is:

$$\rho(X,Y) = \frac{cov(X,Y)}{\sigma_X \sigma_Y} \quad (2)$$

where cov is the covariance, and $\sigma_X \sigma_Y$ is the standard deviation of X and Y.

Furthermore, Friedman and multiple comparison tests with a confidence level of $p<0.05$ was used for the statistical significance check.

III. RESULTS AND DISCUSION

A. Brain Topographical map

The brain topographical map was generated by computing each participant's z-score power across all channels. Fig. 2 presents a representative topographical map of P2. From Fig. 2, strong desynchronization is noticeable for wrist motion tasks (WEMI and WFMI) compared to grasping motion tasks (KGMI and PGMI) for all the TH groups. One possible reason for this could be that grasp tasks involve hand and wrist muscle strength coordination which requires different combinations of movements of the fingers and wrist. In this regard, grasping tasks could be more complex to imagine than wrist movement tasks. PGMI shows the weakest response for all TH groups. Also, lateralization could be seen for all the tasks except for some TH groups in PGMI though with varying response strength. Comparing the response for each task in NO-TH with data preprocessed with different artifactual component rejection TH values, a significant difference in signal desynchronization could be seen for all the TH groups.

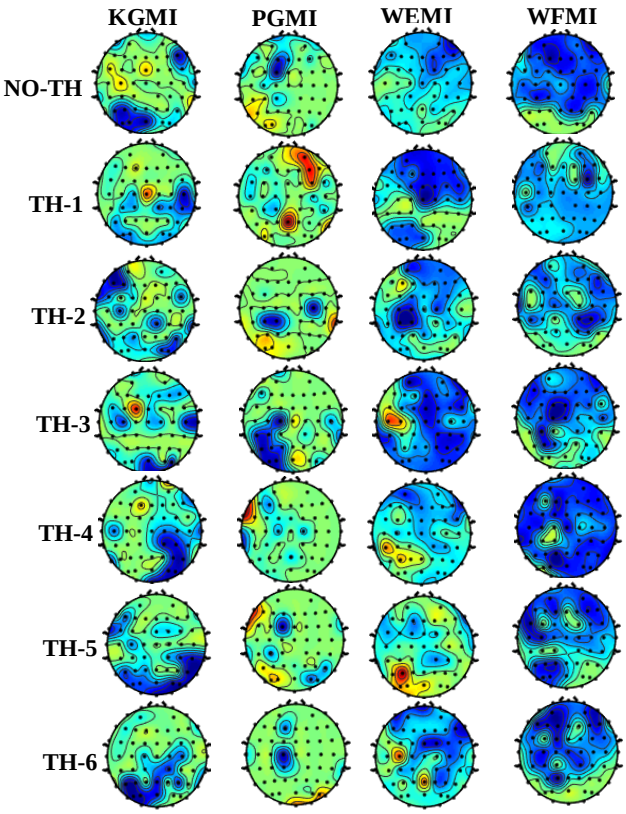

Fig. 2 A representative brain topographical map of patient 2 for all the MI tasks

Again, examining the performance of the TH groups task-wise, TH-2, TH-3, and TH-6 maps show better responses (especially at the ROI) and more appropriate rejection of artifactual ICs. A reduction in brain response is seeable in

PGMI and WEMI tasks for TH-4 and TH-5. Less lateralization in the sensorimotor cortices are found in WEMI and WFMI for TH-1. Based on these results from P2 and other participants (not reported due to pages limitation), it may be concluded that applying TH value with high confidence for ICs rejection in ICLabel classifier may lead to loss of more brain signals, thus affecting the brain signal final pattern. Similarly, utilizing low TH value would allow more artifacts to be retain in the signal.

B. Correlation coefficient analysis

Through a custom-built script in MATLAB, 153 electrode pairs were formed using the eighteen channels at the ROI. After that, the CC (eq. 2) was estimated for each pair of electrodes for all the participants. The Friedman test with p-value < 0.05 was used to evaluate the statistical significance between the TH groups. A multiple comparison test was further use to carry out a pairwise comparison between the groups. The results for each MI task are presented in Fig. 3A-D. The Figure compares the mean of NO-TH (highlighted in blue) and other TH groups. A symbol with a line extending out of it represents each group's mean interval. Two group means are significantly different if their intervals are disjoint and not significant if their intervals overlap. Each plot in Fig. 3A-D shows the result for KGMI, PGMI, WEMI, and WFMI tasks with statistical significance ($p<0.001$) between NO-TH and other TH groups. The TH-3 group shows high and consistent significance for all the tasks except KGMI, where TH-4 is more significant. Based on TH-3 performance, it will be utilized for subsequent result analysis.

All the electrode pair with their respective correlation values could not be reported due to pages limitation, therefore top ten electrode pairs with the highest correlation values for all the tasks in the TH-3 group is presented in Table 3. A high correlation value between the signals from different channel pairs indicates similar brain activity for the specific MI tasks, and a low correlation means the brain signal is relatively independent. Through careful observation, it could be seen that the same electrode pair (C1-CP3) obtained the highest correlation values for KGMI (0.9905), WEMI (0.965), and WFMI (0.9710) tasks, while for PGMI, CP2-CP4 electrode pair has the best correlation values. Overall, more electrode pairs are replicable across the MI tasks. Although P2 has left-hand impairment, electrode pairs' in the bilateral region of the brain show high correlations for the four MI tasks, and ipsilateral regions incline to have more electrode pairs' correlations for KGMI, WEMI, and WEMI probably due to brain reorganization during the recovery.

In addition, all the electrode pairs with high correlation locate closely in the same cortices and few electrode pairs between hemispheres show high correlations. These results reveal that brain activity correlates linearly with distance, and a strong correlation between electrode pairs is independent of the different brain cortices.

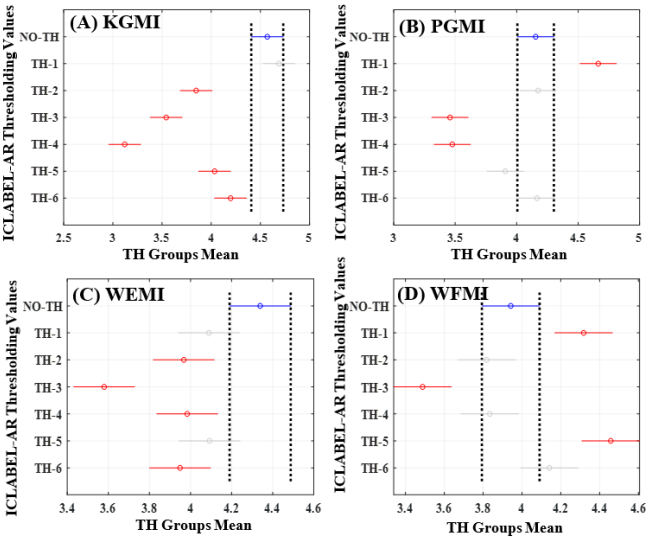

Fig. 3 A multiple comparison plot between the considered TH groups correlation values for (A) KGMI (B) PGMI (C) WEMI and (D) WFMI

C. Evaluation of MI tasks Decoding Performance

The bar plot in Fig. 4A depicts the mean decoding performance across tasks for NO-TH and TH-3 groups. The result present in this Fig. revealed the effect of artifacts contamination in EEG signal on MI tasks classification accuracy. For all the participants, the signal preprocessed with TH-3 performed better than data without ICs artifact rejection TH (Friedman test, $p = 0.01$). Generally, P2 achieved the highest decoding accuracy of $99.39\% \pm 0.52$ followed by P1 ($97.15\% \pm 2.97$). The least performance was obtained by P3 ($69.67\% \pm 9.02$). Specifically TH-3 recorded an increment of 47.19%, 46.66%, 16.79%, 5.02%, 23.02% and 32.16% for P1, P2, P3, P4, P5 and P6 against NO-TH group. The confusion matrix shown in Fig. 4B and 4C represents individual task classification performance across all the participants. Fig. 4B present the result for NO-TH data while 4C for TH-3 result. Inspecting both confusion matrixes, the TH-3 obtained better accuracies for all the tasks with a statistical significance of $p=0.04$. For both groups, the KGMI task has the highest performance.

Table 3: Top ten electrode pair correlation values ranked using correlation coefficient quantifier

S/N	CHAN. PAIRS	KGMI	CHAN. PAIRS	PGMI	CHAN. PAIRS	WEMI	CHAN. PAIRS	WFMI
1	C1-CP3	0.9905	CP2-CP4	0.9216	C1-CP3	0.965	C1-CP3	0.9710
2	C1-CP1	0.9788	FC4-C2	0.8580	CP4-CP6	0.9319	C1-CP1	0.9689
3	CP1-CP3	0.9701	C3-C5	0.8107	FC5-C5	0.9160	CP1-CP3	0.9488
4	CP4-CP6	0.9016	FC5-C3	0.8005	CP1-CP3	0.8929	FC4-FC6	0.9448
5	FC2-C2	0.8490	FC4-FC6	0.7948	FC4-FC6	0.8916	FC3-FC5	0.9379
6	CP2-CP4	0.7505	C1-CP3	0.7868	C1-CP1	0.8884	C3-C5	0.9233
7	FC4-FC6	0.7496	FC2-C2	0.7803	FC2-C2	0.8611	FC2-FC4	0.9227
8	C4-CP2	0.7435	FC6-C6	0.7795	C3-C5	0.8286	FC5-C5	0.9183
9	C4-CP4	0.7298	FC5-C5	0.7733	FC2-FC4	0.8193	FC2-C2	0.9120
10	CP2-CP6	0.7122	FC2-FC4	0.7612	FC3-C3	0.8077	FC5-C3	0.9025

The WEMI task recorded the least accuracy for NO-TH while WFMI for TH-3. It is worth stating that the KGMI results presented in this study were computed using data from 5 participants because P1 couldn't imagine the key grip task during the experiment sessions.

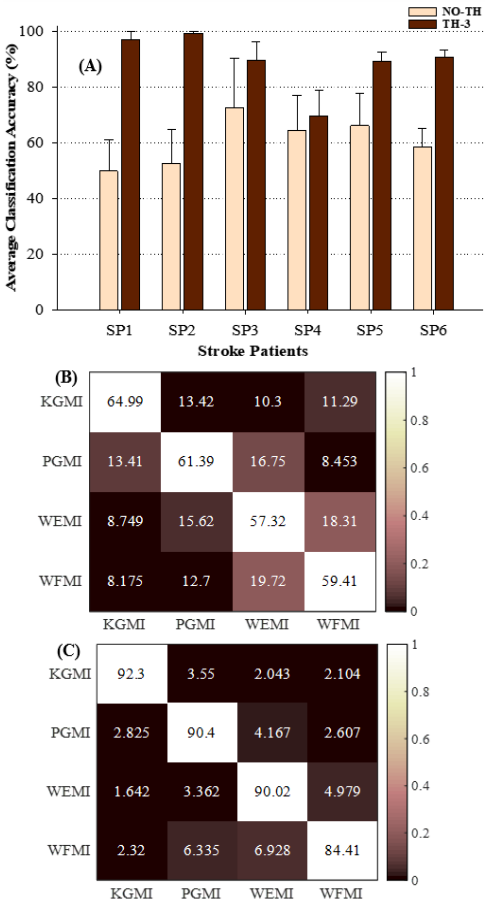

Fig. 4 (A) Subject-wise average classification accuracy across all tasks. Average decoding performance across participants for individual MI tasks for (B) NO-TH group and (C) TH-3 group.

IV. CONCLUSION

This study investigated the impact of varying ICLABEL-based artifact rejection THs on motor cortex beta oscillatory activity from MI-EEG signal recordings in post-stroke survivors. The effects were quantified using three EEG-based metrics and finding from the experimental results revealed that the artifact rejection TH will definitely altered the brain oscillatory pattern. Specifically, some TH values result in increased brain response while some decrease the brain activation response. In the correlation analysis, TH-3 demonstrates consistent and high statistical significance (with NO-TH) for all the tasks compared to others. The result shows that brain activity correlates linearly with distance, and a high correlation value is unrelated or unassociated with the region of the brain. Besides, a high correlation value implies a stronger functional connectivity between different areas of the brain and vice-versa. Therefore, correlation analysis can be used to study the functional connectivity patterns of the brain. The TH-3 data achieved high decoding accuracy subject-wise and in the individual MI decoding. Based on the findings from this work, utilizing TH with a high confidence level may lead to significant loss of brain signal, and a low confidence level can result in less removal of artifacts; therefore, this study will suggest a TH-values between confidence level among the range of 50% - 70%. Notably, the ICLABEL-TH should be selected with caution and according to the study objective(s) to prevent signal misinterpretation. It is worth stating that this is a preliminary finding and is limited in data sample size, EEG frequency band, and rigorous analyses. Extensive research is ongoing to further validate our findings.

REFERENCES

[1] Feigin, V. L., Stark, B. A., Johnson, C. O., Roth, G. A., Bisignano, C., Abady, G. G., ... & Hamidi, S. Global, regional, and national burden of stroke and its risk factors, 1990–2019: a systematic analysis for the Global Burden of Disease Study 2019. The Lancet Neurology, 20(10), 795-820, 2021.

[2] Khallaf, M. E. Effect of task-specific training on trunk control and balance in patients with subacute stroke. Neurology Research International, 2020, 1-8, 2020.

[3] Ingwersen, T., Wolf, S., Birke, G., Schlemm, E., Bartling, C., Bender, G., ... & Thomalla, G. Long-term recovery of upper limb motor function and self-reported health: results from a multicenter observational study 1 year after discharge from rehabilitation. Neurological Research and Practice, 3(1), 1-10,2021.

[4] Espenhahn, S., Rossiter, H. E., van Wijk, B. C., Redman, N., Rondina, J. M., Diedrichsen, J., & Ward, N. S. Sensorimotor cortex beta oscillations reflect motor skill learning ability after stroke. Brain communications, 2(2), fcaa161, 2020.

[5] Leonardi, G., Ciurleo, R., Cucinotta, F., Fonti, B., Borzelli, D., Costa, L., ... & Alito, A. The role of brain oscillations in post-stroke motor recovery: An overview. Frontiers in Systems Neuroscience, 16, 947421,2022.

[6] Milani, G., Antonioni, A., Baroni, A., Malerba, P., & Straudi, S. Relation Between EEG Measures and Upper Limb Motor Recovery in Stroke Patients: A Scoping Review. Brain Topography, 35(5-6), 651-666,2022.

[7] Asogbon, M. G., Samuel, O. W., Li, X., Nsugbe, E., Scheme, E., & Li, G. A linearly extendible multi-artifact removal approach for improved upper extremity EEG-based motor imagery decoding. Journal of Neural Engineering,2021.

[8] Jiang, X., Bian, G. B., & Tian, Z. Removal of artifacts from EEG signals: a review. Sensors, 19(5), 987,2019.

[9] Rejer, I., & Górski, P. (2015, August). Benefits of ICA in the case of a few channel EEG. In 2015 37th Annual International Conference of the IEEE Engineering in Medicine and Biology Society (EMBC) (pp. 7434-7437). IEEE.

[10] Zapata-Saldarriaga, L. M., Vargas-Serna, A. D., Gil-Gutiérrez, J., Mantilla-Ramos, Y. J., & Ochoa-Gómez, J. F. Evaluation of Strategies Based on Wavelet-ICA and ICLabel for Artifact Correction in EEG Recordings. Revista Científica, 46(1), 61-76,2023.

[11] Pion-Tonachini, L., Kreutz-Delgado, K., & Makeig, S.ICLabel: An automated electroencephalographic independent component classifier, dataset, and website. NeuroImage, 198, 181-197,2019.

[12] Bailey, N., Biabani, M., Hill, A. T., Miljevic, A., Rogasch, N. C., McQueen, B. & Fitzgerald, P. Introducing RELAX (the Reduction of Electroencephalographic Artifacts): A fully automated pre-processing pipeline for cleaning EEG data-Part 1: Algorithm and Application to Oscillations. BioRxiv, 2022-03, 2022.

[13] Vourvopoulos, A., Jorge, C., Abreu, R., Figueiredo, P., Fernandes, J. C., & Bermudez i Badia, S. Efficacy and brain imaging correlates of an immersive motor imagery BCI-driven VR system for upper limb motor rehabilitation: A clinical case report. Frontiers in human neuroscience, 13, 244, 2019.

[14] Mansor, W., Abd Rani, M. S., & Wahy, N. Integrating neural signal and embedded system for controlling small motor. InTech, 2011.

[15] Ray, A. M., Figueiredo, T. D., López‐Larraz, E., Birbaumer, N., & Ramos‐Murguialday, A. Brain oscillatory activity as a biomarker of motor recovery in chronic stroke. Human brain mapping, 41(5), 1296-1308,2020.

[16] Akin, M. Comparison of wavelet transform and FFT methods in the analysis of EEG signals. Journal of medical systems, 26, 241-247,2002.

[17] Amin, H. U., Malik, A. S., Ahmad, R. F., Badruddin, N., Kamel, N., Hussain, M., & Chooi, W. T. Feature extraction and classification for EEG signals using wavelet transform and machine learning techniques. Australasian physical & engineering sciences in medicine, 38, 139-149,2015.